Energy Reports 7 (2021) 8013–8020

Contents lists available at ScienceDirect

Energy Reports

journal homepage: www.elsevier.com/locate/egyr

# Geomechanical properties of gas hydrate-bearing sediments in Shenhu Area of the South China Sea

Jiangong Wei [a,b,c], Lin Yang [a,b,*], Qianyong Liang [a,b], Jinqiang Liang [a,b], Jingan Lu [a,b], Wei Zhang [a,b], Xuhui Zhang [d,**], Xiaobing Lu [d]

[a] Guangzhou Marine Geological Survey, China Geological Survey, Guangzhou 510075, China
[b] Gas Hydrate Engineering Technology Center, China Geological Survey, Guangzhou 510075, China
[c] Southern Marine Science and Engineering Guangdong Laboratory (Guangzhou), Guangzhou, 511458, China
[d] Institute of Mechanics, Chinese Academy of Sciences, Beijing, 100190, China

ARTICLE INFO

*Article history:*
Received 24 March 2021
Received in revised form 9 May 2021
Accepted 29 May 2021
Available online 10 June 2021

*Keywords:*
Natural gas hydrate
Pressure core
Effective stress
Shear strength
Permeability anisotropy

ABSTRACT

It is essential to understand the in-situ geomechanical properties of natural gas hydrate-bearing reservoirs for hydrate drilling, the design of reservoir stimulation and production schemes, geologic disaster prevention, and environmental impact assessment. In this way, it serves as the basis for the development and utilization of gas hydrate resources. In 2016, the Guangzhou Marine Geological Survey conducted the fourth natural gas hydrate drilling (Expedition GMGS4) in the north of the South China Sea, during which the effective stress of gas hydrate-bearing reservoirs in the study area was ascertained and gas hydrate-bearing pressure cores were collected. The effective stress was determined to be 700–800 kPa by in-situ piezocone penetration tests. The saturation, permeability, and shear strength of gas hydrates in the pressure core samples were measured under the in-situ stress state using the shipboard multi-sensor core logger (MSCL), pressure core analysis and transfer system (PCATS), and PCATS Triaxial system. Based on this, the distribution characteristics and the relationship of the permeability and gas hydrate saturation of the gas hydrate-bearing reservoirs were explored. Furthermore, the effects of effective stress and gas hydrate saturation on shear strength of gas hydrate-bearing clayey-silt sediments were mainly analyzed, as well as the stress–strain characteristics of gas hydrate-bearing sediments. The results are as follows: (i) the gas hydrate saturation and reservoir permeability in the study area are 0.7%–55% and $10^{-3}$–$10^{-1}$ mD, respectively, indicating low-permeability reservoirs; (ii) the gas hydrate saturation and reservoir permeability have obvious anisotropy in horizontal and vertical directions; (iii) the undrained shear strength of gas hydrate-bearing sediments is 0.24–0.52 MPa, and the shear strength of fine-grained sediments is more sensitive to the changes of in-situ stress. In the case that deviatoric stress continues increasing, micro-fractures may occur inside gas hydrate-bearing sediments, and this can lead to drastic changes in the strength of gas hydrate-bearing reservoirs. Therefore, it is necessary to take into account the effects of micro-fractures in gas hydrate-bearing reservoirs on engineering safety during long-term hydrate production.



## 1. Introduction

Natural gas hydrates (NGHs) are widely distributed in offshore continental slope sediments and permafrost zones. They are recognized as one of the most promising clean energy sources in the 21st century owing to their considerable resource potential, high energy density, and low environmental pollution (Collett, 2002; Solan, 2003; Boswell, 2009). NGHs are widely distributed all over the world, with 90% of the ocean serving as potential areas for NGH deposits (Johnson, 2011; Max and Johnson, 2016; Wei et al., 2015, 2019, 2021). Marine NGHs are mostly formed in pores or fractures in submarine sediments, which serve as an important part of the gas hydrate-bearing reservoir matrix and have significant impacts on the geomechanical properties of NGH reservoirs, such as pore structure, seepage characteristics, strength, and stiffness (Phillips, 1991; Song et al., 2014; Lu et al., 2019; Zhu et al., 2019, 2020). In the long-term production of NGHs, the dissociation of a large number of gas hydrates will reduce the geomechanical strength of gas hydrate-bearing reservoirs, cause reservoir deformation, and even

* Corresponding author at: Guangzhou Marine Geological Survey, China Geological Survey, Guangzhou 510075, China.
** Corresponding author.
*E-mail addresses:* yl_gmgs@163.com (L. Yang), zhangxuhui@imech.ac.cn (X. Zhang).

https://doi.org/10.1016/j.egyr.2021.05.063

trigger submarine geologic disasters such as stratum collapse and submarine landslides (Zhang et al., 2015b; Wang et al., 2020). Therefore, it is essential to understand the geomechanical properties of gas hydrate-bearing reservoirs for production scheme design, gas hydrate-bearing reservoir stability assessment, and geologic disaster prevention during long-term gas hydrate production (Boswell et al., 2019; Zhang et al., 2019; Qin et al., 2020).

The structure and morphology are important parameters to effect the geomechanical properties of gas hydrate-bearing sediments (Waite et al., 2009; Holland et al., 2019; Lijith et al., 2019). Gas hydrate dissociated will produce large number of gas, which enhanced pore pressure and reduced effect stress. The structure and morphology of gas hydrate-bearing sediments are changed, that the geomechanical properties of depressurized gas hydrate-bearing sediments cannot reflect that of gas hydrate reservoirs. On the other hand, the structure of laboratory reconstituted hydrate samples is also difference from that of hydrate reservoirs (Li et al., 2019; Dong et al., 2020). Therefore, the geomechanical properties of in-situ gas hydrate-bearing sediments is important.

In 2017 and 2020, the China Geological Survey conducted offshore NGH production tests twice in Shenhu area, South China Sea. As shown by the monitoring results of these production tests, short-term NGH production test will not cause geologic disasters such as stratum collapse and submarine landslides; however, the assessment of submarine stratum stability during long-term production is still a key issue to be addressed (Li et al., 2018; Ye et al., 2018, 2020). As for the gas hydrate-bearing reservoirs in the production test area in the South China Sea, there are a few studies on the geomechanical properties of the gas hydrate-bearing clayey-silt reservoirs (Shi et al., 2015; Zhang et al., 2015a; Lu et al., 2017; Wang et al., 2018) and fewer geomechanical property data of in-situ or low-disturbed gas hydrate-bearing pressure cores (Liang et al., 2017). Furthermore, as the NGHs in the South China Sea mainly occur in non-diagenetic submarine sediments, the geomechanical properties of gas hydrate-bearing sediments are prone to be affected by temperature, pore pressure, effective stress, and sediment structure. Therefore, the results of in-situ or low-disturbed gas hydrate-bearing pressure cores are more favorable for the reflection of original geomechanical properties of NGH reservoirs (Yoneda et al., 2015b; Jang et al., 2019; Yoneda et al., 2019b).

In 2016, the Guangzhou Marine Geological Survey conducted the fourth NGH drilling (Expedition GMGS4) project (Fig. 1) in the South China Sea to research the geomechanical properties of the gas hydrate-bearing reservoirs in the NGH production test area in the South China Sea (also referred to as the study area). During the project, the effective stress of gas hydrate-bearing reservoirs in the study area was ascertained and gas hydrate-bearing pressure core samples were collected. The gamma density, compressional wave (P-wave) velocity, gas hydrate saturation, permeability, and shear strength of the pressure core samples were measured using a MSCL, PCATS, and PCATS Triaxial system. Based on this, the distribution characteristics and the relationship between the permeability and gas hydrate saturation of gas hydrate-bearing reservoirs in the study were explored. Furthermore, the effects of effective stress and gas hydrate saturation on shear strength of gas hydrate-bearing clayey-silt sediments were mainly analyzed, as well as the stress–strain characteristics of gas hydrate-bearing sediments.

## 2. Pressure core samples from expedition GMGS4

The drilling area of Expedition GMGS4 is located in Shenhu Area, northern South China Sea. As indicated by logging while drilling (LWD) data as well as drilling and coring data, the NGHs encountered were mainly disseminated hydrates occurring in clayey-silt-dominated sediments at a depth of approximately 116.5–265 mbsf, with a water depth of 1000–1400 m. The fines content (the grain size less than 0.075 mm) is about 95%–100%, a median grain size (MZ) of about 4–28.76 μm, and the mean median grain size of the sediments is about 12 μm. The minerals are mainly quartz-feldspathic (53%), carbonates (16%) and clay minerals (26%–30%), which are mainly montmorillonite and illite, and methane content of more than 93.5% (Yang et al., 2015; Li et al., 2018; Wei et al., 2018; Zhang et al., 2020). This area features a seafloor temperature of 3.3–3.7 °C, a geothermal gradient of 45–67 °C/km, and the NGH reservoirs temperature of about 6.3–9.0 °C (Zhang et al., 2017). A certain number of pressure core samples were collected from the study area using a pressure coring tool with ball valve (PCTB, FUGRO N.V.) during the Expedition GMGS4 (Schultheiss et al., 2011; Yang et al., 2017; Holland et al., 2019). Then geomechanical tests were carried out on seven pressure core samples from four sites (SC-W01B, SC-W01C, SC-W02B, and SH-W07b) using the PCATS. The water depth of the drilling area is about 914–1287 m (Fig. 2A), and the sampling depth is 137.59–159.91 mbsf (Fig. 2B).

The pressure core samples were transferred from PCTB to the PCATS Triaxial system while retaining their pressure, followed by non-destructive scanning of the samples. As for the samples meeting quality requirements according to the nondestructive scanning, their gamma density and P-wave velocity were determined using the MSCL, which serve as the basis for the analysis of hydrate-rich areas of the samples. Afterwards, the segmentation scheme of the samples was determined. Finally, the samples were cut into an 11 cm long subsamples (core diameter: 53 mm) according to the scan and analysis results while retaining their pressure.

As shown in Fig. 2, the gamma density, corresponding porosity, and P-wave velocity of the subsamples are 1.57–1.73 g/cm$^3$ (Fig. 2C), 58%–64% (Fig. 2D), and 1575–2394 m/s (Fig. 2E), respectively, and the gamma density of the sediments is positively correlated with their porosity. The hydrate saturation of the subsamples was determined to be 0.7%–55% by depressurization and gas-release tests (Fig. 2F).

## 3. Test methods

### 3.1. Depressurization and gas-release tests

The depressurization and gas-release tests were designed to measure the gas hydrate saturation in the pressure core samples in order to characterize the hydrate distribution in NGH reservoirs. Based on this, the relationship of gas hydrate saturation with P-wave velocity and permeability can be analyzed through the P-wave velocity scanning and permeability tests of the pressure core samples. Two subsamples (SC-W01B-8A-8 and SC-W01B-14A-6) with P-wave velocity close to 1500 m/s were selected according to the P-wave velocity scanning results as non-hydrate (low-saturation) samples for comparative analysis.

During the depressurization and gas release, the effective stress of the pressure core samples was maintained as positive to avoid sample motion. In order to control the hydrate dissociation in this test, the step-down depressurization method is used. First, depressurized the pressure close to the hydrate equilibrium pressure fast. When the pressure below to the equilibrium pressure, control the depressurized rate at dozens or hundreds of kPa. Then, collect the gas and closed the valve until the pressure rise to equilibrium pressure. And repeat the operation until the end of hydrate dissociation. The gas collection device consisted of a water tank used to record water level and an inverted measuring cylinder full of water. At a temperature of 8 °C and

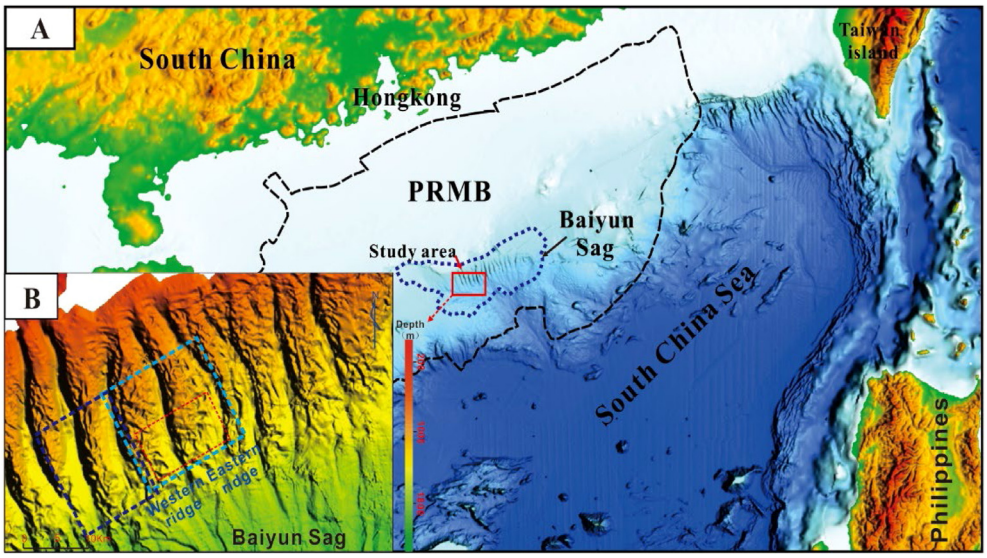


**Fig. 1.** Geographical location map of the study area of Expedition GMGS4 in the South China Sea.

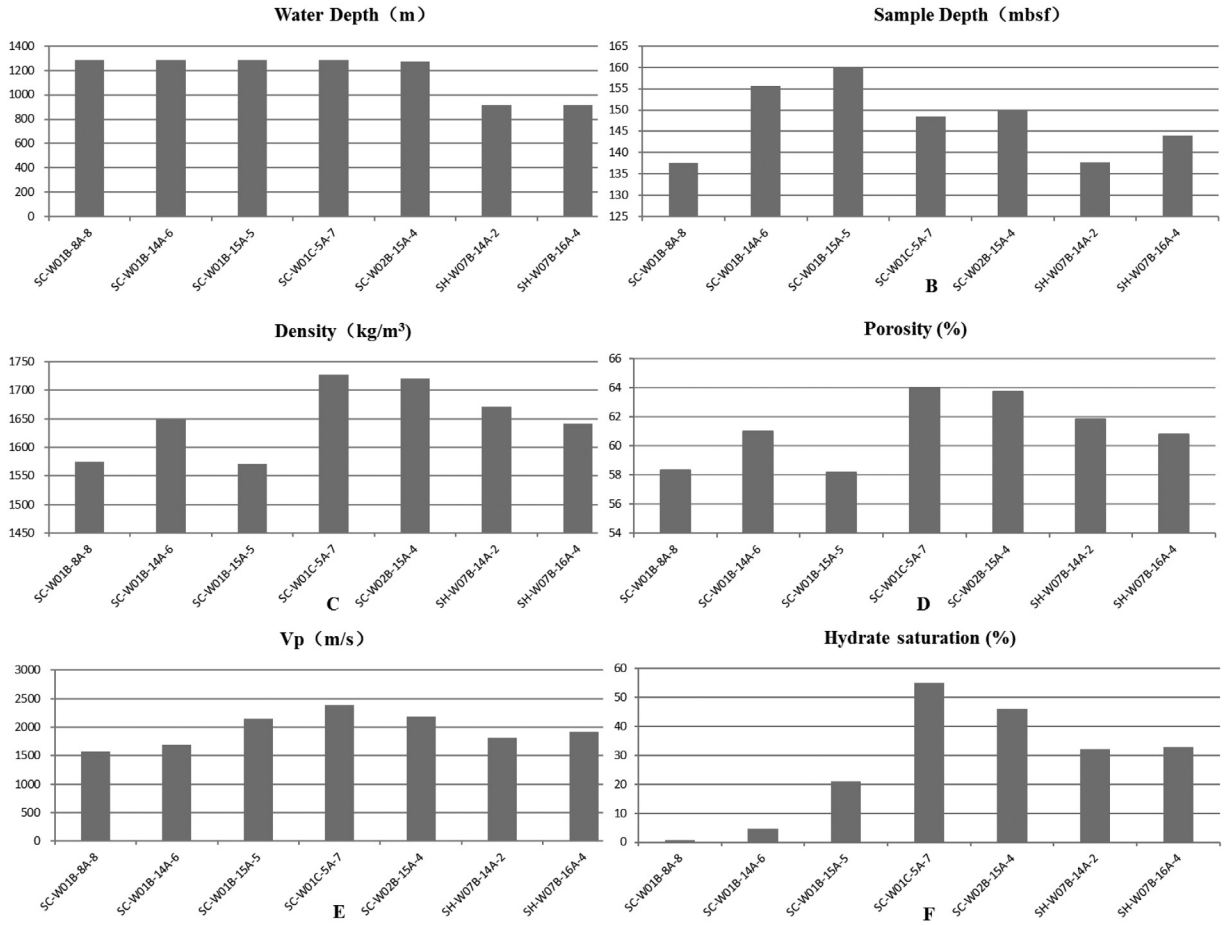


**Fig. 2.** Occurrence characteristics and basic physical property parameters of pressure core samples (SC-W01B-8A-8, SC-W01B-14A-6, SC-W01B-15A-5, SC-W01B-5A-7, SC-W02B-15A-4, SH-W07B-14A-2 and SH-W07B-16A-4). (A) Water depth; (B) Sampling depth; (C) Gamma density; (D) Porosity; (E) P-wave velocity; (F) Hydrate saturation.

standard atmospheric pressure, fluids (including gas and water) entered the measuring cylinder through a gas release valve. The gas volume and water volume were obtained by measuring the gas volume in the measuring cylinder and the water level increment in the water tank, respectively. The hydrate content was calculated based on the gas volume. The results of Raman analysis showed that the hydration index of the pressure core samples from Expedition GMGS4 is 6 (Wei et al., 2018). The gas hydrate saturation was defined as the percentage of the hydrate volume accounting for the pore volume of the sediments, and the

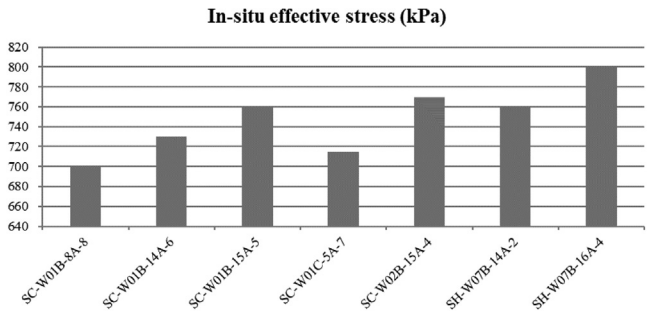


**Fig. 3.** In-situ effective stress of the gas hydrate-bearing reservoirs of the pressure core samples (SC-W01B-8A-8, SC-W01B-14A-6, SC-W01B-15A-5, SC-W01C-5A-7, SC-W02B-15A-4, SH-W07B-14A-2, and SH-W07B-16A-4).

porosity of gas hydrate-bearing reservoirs was measured by LWD and core scanning.

### 3.2. Permeability tests

The permeability tests were designed to measure the permeability of the pressure core samples under in-situ effective stress condition of gas hydrate-bearing reservoirs, in order to analyze the response of reservoir permeability to gas hydrate saturation. Stepwise increase of effective stress was adopted until in-situ effective stress was obtained (Yoneda et al., 2019a). A pressurization stage ended when the total volume of liquid seeping out of the pressure core samples became constant and then the next pressurization stage started. The effective stress of gas hydrate-bearing reservoirs was determined to be 700–800 kPa (Fig. 3) by in-situ cone penetration tests (CPT). After the in-situ effective stress was obtained, permeability tests were carried out under constant effective stress. Pressure/volume controllers were employed to keep the fluids flowing upwards at a constant flow rate of 100 nL/s. The pore pressure at the top and bottom of the samples was monitored, and the vertical permeability of the samples was calculated according to Darcy's Law once a hydraulic gradient became constant.

### 3.3. Compression tests

The compression tests were carried out on the pressure core samples collected from gas hydrate-bearing clayey-silt reservoirs using the shipboard PCATS Triaxial system. They were designed to measure the shear strength of the original gas hydrate-bearing reservoirs and analyze the stress–strain relationship of the pressure core samples. The samples SC-W02B-15A-4 and SC-W01B-15A-5 were tested under the effective confining pressure of 1200 kPa and 2200 kPa, respectively. The effective confining pressure is bore by pore fluid and soil skeleton, which equals the difference between the total confining pressure and pore pressure. And the remaining five samples were tested under in-situ effective stress.

The axial strain tests were performed at an axial deformation rate of 1%/min, during which the deviatoric stress ($q$) was recorded. The axial deformation rate remained unchanged after an sample was destroyed until the drive device reached its maximum torque. When the sample exhibited strain-softening, the peak value of the deviatoric stress was taken as the shear strength. Otherwise, the deviatoric stress ($q$) at the local minimum of the average effective stress ($p$') was taken as the shear strength (Yoneda et al., 2019b).

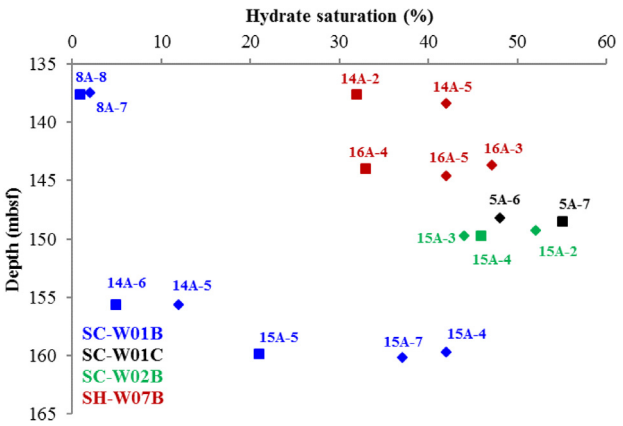


**Fig. 4.** Distribution characteristics of gas hydrate saturation in the drilling area of Expedition GMGS4. Note: the squares represent the triaxial test data, and the diamonds denote the gas hydrate saturation obtained from direct dissociation of gas hydrates in the reservoirs of similar strata.

## 4. Results and discussion

### 4.1. Gas hydrate saturation

Gas hydrate saturation is an important parameter controlling the effective permeability and geomechanical strength of gas hydrate-bearing sediments (Yoneda et al., 2015b; Zhang et al., 2016). The gas hydrate saturation of gas hydrate-bearing reservoirs and pressure core samples can be effectively determined by two means, namely P-wave scanning and depressurization and gas-release tests (Ning et al., 2012; Wei et al., 2018; Ye et al., 2019). For gas hydrate-bearing clayey-silt sediments, (Holland et al., 2019) found that the sediments contain no or only a small number of hydrates when their P wave velocity was about 1500 m/s, while they are reservoirs with high gas hydrate saturation when their P-wave velocity is 2000–3300 m/s. According to the P-wave scanning and depressurization and gas-release tests of the pressure core samples taken from the gas hydrate-bearing clayey-silt sediments in the study area, the P-wave velocity of the samples is 1575–2394 m/s and the corresponding gas hydrate saturation is 0.7%–55% (Fig. 2E, F), thus verifying the relationship between the P-wave velocity and gas hydrate saturation of gas hydrate-bearing clayey-silt sediments in the study area.

As shown in Fig. 4, the gas hydrate saturation of Site SC-W01B is significantly different in the vertical direction, varying from 0.7% to 42%. According to the comparison among the gas hydrate saturation of different sites with a similar depth, the gas hydrate saturation also shows obvious differences in the horizontal direction. The gas hydrate saturation of the gas hydrate-bearing reservoirs at a depth of about 137 mbsf, 145–150 mbsf, and 155–160 mbsf is 0.7%–42%, 33%–55%, and 33%–42%, respectively. Therefore, the hydrate saturation in the study area has obvious anisotropy. The hydrate saturation is an important parameter to evaluate the permeability and the geomechanical properties of NGHs reservoir. In different hydrate saturation conditions, the gas production rate and the hydrate dissociation behaviors are not the same. Therefore, the area which hydrate saturation has obvious anisotropy is the major area to evaluate the NGHs reservoirs stability.

### 4.2. Permeability

The NGHs encountered in the drilling area of Expedition GMGS4 were concluded to be disseminated and were hosted in the clayey-silt-dominated sediments. In this study, permeability

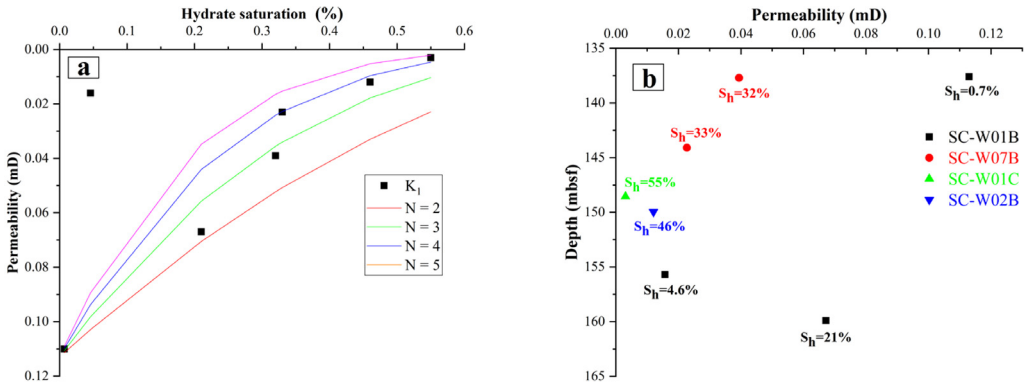


**Fig. 5.** (a) Relationship between permeability and gas hydrate saturation of the pressure core samples. (b) Relationship between the permeability and burial depth of the pressure core samples. **Note**: $K_1$ is the tested permeability of the samples. The curves present the relationships between the calculated permeability and gas hydrate saturation of the samples when $N = 2$, 3, and 4.

tests were carried out on seven pressure core samples taken from the clayey-silt sediments to analyze the relationship of the permeability of the sediments with gas hydrate saturation and burial depth. Among these seven samples, the sample SC-W01B-8A-8 has gas hydrate saturation of only 0.7%, almost bearing no hydrates. Therefore, its permeability was taken as the initial permeability of the host sediments. As shown from Fig. 5a to b, the permeability of the samples decreases with an increase in gas hydrate saturation, which is consistent with the relationship between the permeability and gas hydrate saturation of gas hydrate-bearing porous media. However, the sample SC-W01B-14A-6 has abnormal permeability, which may be caused by the blockage of seepage channels. As a result, it was excluded from this study. As shown in Fig. 6, the permeability of the remaining samples is mainly $10^{-3}$–$10^{-1}$ mD, but shows obvious anisotropy in both horizontal and vertical directions. The permeability of NGHs reservoirs is a very important parameter to analyze the gas production rate, heat and mass transfer efficiency. By considering the anisotropy in permeability of NGHs reservoir, it can be get the more accurately predicted results about gas hydrate dissociation behaviors in gas hydrate production process.

It has been concluded that the corresponding relationship between the porosity and permeability of porous media is as follows (Phillips, 1991); Eq. (1):

$$K_1 = K_0\left(\frac{\varphi_1}{\varphi_0}\right)^N \tag{1}$$

where, $K_0$ and $\varphi_0$ are the initial permeability and porosity of the porous media, respectively; $K_1$ and $\varphi_1$ are the absolute permeability and porosity of the porous media after the porosity changes, respectively; $N$ is permeability reduction index, about 2–3. Based on Eq. (1), Masuda (1999) deduced and verified the relationship between gas hydrate saturation and absolute permeability of gas hydrate-bearing sandstone (Eq. (2)):

$$K_1 = K_0(1 - S_h)^N \tag{2}$$

where, $K_0$ and $K_1$ are the initial and absolute permeability of gas hydrate-bearing sandstone, $S_h$ is gas hydrate saturation, and $N$ is about 2–4.4 (Konno et al., 2010).

$N$ was calculated to be 2.2–4.5 by substituting the initial permeability and gas hydrate saturation of host sediments in the study area and the permeability of the samples into Eq. (2). Moreover, $N$ tended to increase as the hydrate saturation increased, which is similar to the results of coarse-grained sediments (Konno et al., 2010). The curves of the relationship between permeability and gas hydrate saturation of the samples were plotted by taking $N = 2$, 3, 4, and 5 (Fig. 5a). Where $S_h = 21\%$, the permeability calculated using $N = 2$ is close to the tested permeability. Where $S_h = 32\%$–$46\%$, the permeability curves of $N = 3$ and 4 fit the measured data better. Where $S_h = 55\%$, the permeability calculated using $N = 4$ and 5 are closer to the tested permeability. The reason for these results is that the pore volume of the sediments decreases as the gas hydrate saturation increases. After the seepage channels are compressed, the impacts of frictional resistance of particles and bound water on the seepage characteristics of the sediments rapidly increase. This leads to a more significant response of the permeability of gas hydrate-bearing porous media to the increase of gas hydrate saturation. Therefore, $N$ may change in case of different gas hydrate saturation (low, medium, and high saturation). More detailed corresponding relationship is yet to be further studied.

### 4.3. Shear strength and stress–strain characteristics

As shown in Fig. 6, the shear strength of the pressure core samples tested under in-situ effective stress is 0.24–0.52 MPa. When the effective confining pressure was increased to 1200 kPa and 2200 kPa, the shear strength of samples SC-W02B-15A-4 and SC-W01B-15A-5 was increased to 1.1 MPa. As shown in Fig. 6a, for the fine-grained clayey-silt sediments in the study area, the increase in hydrate saturation will lead to an increase in the shear strength of the sediments. This is similar to the test results of remolded gas hydrate-bearing clayey-silt sediments (Zhang et al., 2015b). In the similar confining pressure conditions, the shear strength of in-situ gas hydrate-bearing sediments are bigger than that of laboratory reconstituted samples. This is because, the sediments structure has an important effect to the shear strength of gas hydrate-bearing sediments. This is also consistent with the relationship between the shear strength and gas hydrate saturation of the gas hydrate-bearing porous media that were individually taken from the first offshore hydrate production test area in Nankai Trough (Yoneda et al., 2015b, 2017) and the study area of Expedition NGHP-02 (Yoneda et al., 2019b). However, compared to coarse-grained gas hydrate-bearing sediments, the gas hydrate saturation produces far smaller effects on the shear strength of fine-grained gas hydrate-bearing sediments.

By comparison with the shear strength of gas hydrate-bearing sediments in different areas in Fig. 6b (Yoneda et al., 2010, 2015a,b; Zhang et al., 2018; Yoneda et al., 2019b), the shear strength of fine-grained gas hydrate-bearing sediments is more sensitive to effective confining pressure than to hydrate saturation. However, for coarse-grained gas hydrate-bearing sediments, gas hydrate saturation has more significant effects than confining pressure. This indicates that the structure and stress condition of host sediments produce more significant effects on the strength

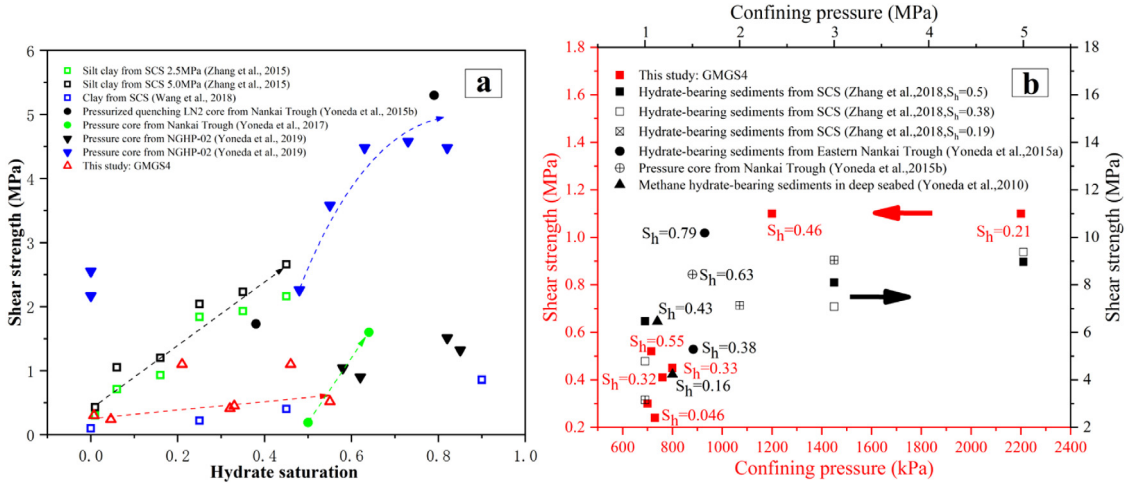


**Fig. 6.** Effects of gas hydrate saturation and effective stress on the shear strength of gas hydrate-bearing clayey-silt sediments in the study area. (a) Relationship between gas hydrate saturation and shear strength of gas hydrate-bearing sediments; (b) Trends of the shear strength of gas hydrate-bearing sediments varying with different effective stress or confining pressure.

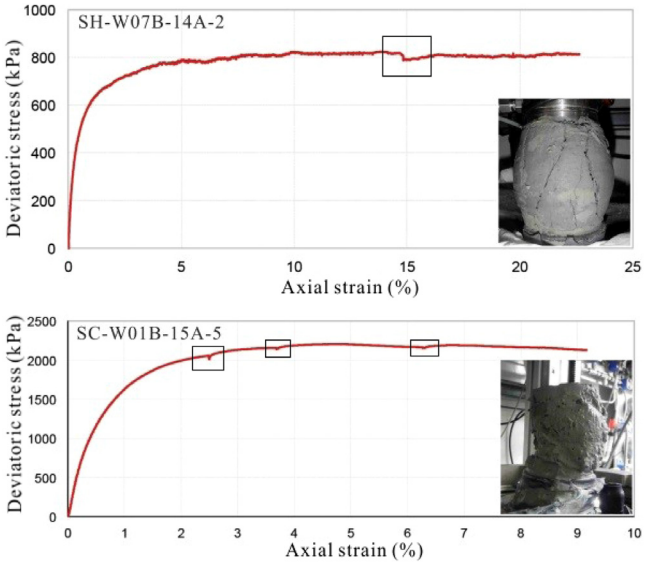


**Fig. 7.** Relationship between deviatoric stress and axial strain in the process of compression tests.

of the fine-grained gas hydrate-bearing sediments than on the strength of coarse-grained gas hydrate-bearing sediments.

The pressure core samples exhibited strain softening with an increase in deviatoric stress, which was typical plastic deformation. Three points with distinct stress decrease can be observed in the sample SC-W01B-15A-5 as the strain increased, but their stress immediately returned to the original values (Fig. 7). This is due to the anisotropy of the mechanical properties (e.g., modulus and strength) of deep-sea fine-grained gas hydrate-bearing sediments. The samples are prone to produce micro-fractures as deviatoric stress increases. However, the particles in the sediments are quickly rearranged to continue providing support to restore the deviatoric stress to its original values.

## 5. Conclusions

For the gas hydrate-bearing reservoirs in the study area of Expedition GMGS4, the effective stress is 700–800 kPa, the gas hydrate saturation ranges between 0.7% and 55%, and the permeability is mainly $10^{-3}$–$10^{-1}$ mD, indicating low-permeability reservoirs. Meanwhile, the gas hydrate saturation and permeability have obvious anisotropy in horizontal and vertical directions.

The permeability reduction index in the study area is 2.2–4.5, which tends to increase as hydrate saturation increases. This indicates that the higher the hydrate saturation, the bigger effects of it on the reservoir permeability and that reservoirs with high gas hydrate saturation have low permeability.

The pressure core samples exhibited strain-softening in the study area as the deviatoric stress increased. According to the tests under in-situ stress, the shear strength of the samples is 0.24–0.52 MPa. Moreover, compared to coarse-grained gas hydrate-bearing sediments, the shear strength of fine-grained gas hydrate-bearing sediments is more sensitive to the changes of effective stress. This indicates that the structure and stress condition of host sediments have more significant effects on the strength of the fine-grained gas hydrate-bearing sediments than on the strength of coarse-grained gas hydrate-bearing sediments. Furthermore, micro-fractures may occur in gas hydrate-bearing reservoirs when deviatoric stress continues increasing, leading to drastic changes in the strength of gas hydrate-bearing reservoirs. Therefore, it is necessary to take into account the impacts of micro-fractures in gas hydrate-bearing reservoirs on the safety of drilling and production engineering during long-time hydrate production.

## Declaration of competing interest

The authors declare that they have no known competing financial interests or personal relationships that could have appeared to influence the work reported in this paper.

## Acknowledgments

This study was supported by National Key Research and Development Program of China (No. 2018YFC0310000), Key Special

Project for Introduced Talents Team of Southern Marine Science and Engineering Guangdong Laboratory (Guangzhou), China (GML2019ZD0201), the Major Program of National Natural Science Foundation of China (No. 51991365), the gas hydrate program initiated by the China Geological Survey (No. DD20190218), and the Major Program of Guangdong Basic and Applied Research, China (No. 2019B030302004). We would like to extend our sincere gratitude to Nikolaus Bigalke, John Roberts, P Schultheissd, and M Holland for their field tests and discussion. Our thanks also go to the crew and scientists involved in the Expedition GMGS4 for their assistance in obtaining samples, experimental tests.

## References

Boswell, R., 2009. Is gas hydrate energy within reach?. Science 325, 957–958.
Boswell, R., Myshakin, E., Moridis, G., Konno, Y., Collett, T.S., Reagan, M., Ajayi, T., Seol, Y., 2019. India national gas hydrate program expedition 02 summary of scientific results: Numerical simulation of reservoir response to depressurization. Mar. Pet. Geol. 108, 154–166.
Collett, T.S., 2002. Energy resource potential of natural gas hydrates. AAPG Bull. 86, 1971–1992.
Dong, L., Li, Y., Liao, H., Liu, C., Chen, Q., Hu, G., et al., 2020. Strength estimation for hydrate-bearing sediments based on triaxial shearing tests. J. Pet. Sci. Eng. 184, 106478.
Holland, M.E., Schultheiss, P.J., Roberts, J.A., 2019. Gas hydrate saturation and morphology from analysis of pressure cores acquired in the bay of bengal during expedition NGHP-02, offshore India. Mar. Pet. Geol. 108, 407–423.
Jang, J., Dai, S., Yoneda, J., Waite, W.F., Stern, L.A., Boze, L.-G., Collett, T.S., Kumar, P., 2019. Pressure core analysis of geomechanical and fluid flow properties of seals associated with gas hydrate-bearing reservoirs in the krishna-godavari basin, offshore India. Mar. Pet. Geol. 108, 537–550.
Johnson, A.H., 2011. Global resource potential of gas hydrate-A new calculation. In: The 7th International Conference on Gas Hydrates Edinburgh, Scotland, United Kingdom.
Konno, Y., Oyama, H., Nagao, J., Masuda, Y., Kurihara, M., 2010. Numerical analysis of the dissociation experiment of naturally occurring gas hydrate in sediment cores obtained at the Eastern Nankai Trough, Japan. Energy Fuels 24, 6353–6358.
Li, Y., Hu, G., Wu, N., Liu, C., Chen, Q., Li, C., 2019. Undrained shear strength evaluation for hydrate-bearing sediment overlying strata in the shenhu area, northern south China sea. Acta Oceanol. Sin. 38, 114–123.
Li, J., Ye, J., Qin, X., Qiu, H., Wu, N., Lu, H., Xie, W., Lu, J., Peng, F., Xu, Z., Lu, C., Kuang, Z., Wei, J., Liang, Q., Lu, H., Kou, B., 2018. The first offshore natural gas hydrate production test in South China Sea. China Geol. 1, 5–16.
Liang, J., Wei, J., Bigalke, N., Roberts, J.A., Schultheiss, P.J., Holland, .M.E., 2017. Laboratory quantification of geomechanical properties of hydrate-bearing sediments in the shenhu area of the south China sea at in-situ conditions. In: The 9th International Conference on Gas Hydrates. Denver, Colorado, USA.
Lijith, K.P., et al., 2019. A comprehensive review on bearing sediments. Mar. Pet. Geol. 104, 270–285.
Lu, X., Zhang, X., Shi, Y., Wang, S., Luo, D., 2017. Mechanical properties of hydrate-bearing silty-clay and stress-strain relation. Period. Ocean Univ. China 47, 9–13, (in Chinese with English abstract).
Lu, X., Zhang, X., Wang, S., 2019. Advances on the safety related with natural gashydrate exploitation. Sci. Sin. Phys. Mech. Astron. 49, 034602, (in Chinese with English abstract).
Masuda, Y., 1999. Modeling and experimental studies on dissociation of methane gas hydrate in Berea sandstone core. In: Proceedings of the 3rd international conference on gas hydrates.
Max, M., Johnson, A., 2016. Exploration and Production of Oceanic Natural Gas Hydrate: Critical Factors for Commercialization. Springer, Basel, Switzerland, p. 405.
Ning, F., Yu, Y., Kjelstrup, S., Vlugt, T.J.H., Glavatskiy, K., 2012. Mechanical properties of clathrate hydrates: status and perspectives. Energy Environ. Sci. 5 (6779).
Phillips, O.M., 1991. Flow and Reactions in Permeable Rocks. Cambridge University Press, Cambridge, New York, Melbourne.
Qin, X., Liang, Q., Ye, J., Yang, L., Qiu, H., Xie, W., 2020. The response of temperature and pressure of hydrate reservoirs in the first gas hydrate production test in South China Sea. Appl. Energy 278, 115649.
Schultheiss, P.J., Holland, .M.E., Roberts, J.A., Huggett, Q., Druce, M., Fox, P., 2011. PCATS: pressure core analysis and transfer system. In: The 7th International Conference on Gas Hydrate (ICGH 2011), Edinburgh, Scotland, United Kingdom.
Shi, Y., Zhang, X., Lu, X., Wang, S., Wang, A., 2015. Experimental study on the static mechanical properties of hydrate-bearing silty-clay in the south China sea. Chin. J. Theor. Appl. Mech. 47, 521–528, (in Chinese with English abstract).
Solan, E.D., 2003. Fundamental principles and applications of natural gas hydrates. Nature 426, 353–363.
Song, Y., Zhu, Y., Liu, W., Zhao, J., Li, Y., Chen, Y., Su, Z., Lu, Y., Ji, C., 2014. Experimental research on the mechanical properties of methane hydrate-bearing sediments during hydrate dissociation. Mar. Pet. Geol. 51, 70–78.
Waite, W., Santamarina, J., Cortes, D., et al., 2009. Physical properties of hydrate-bearing sediments. Rev. Geophys. 47, RG4003.
Wang, Y., Kou, X., Feng, J., Li, X., Zhang, Y., 2020. Sediment deformation and strain evaluation during methane hydrate dissociation in a novel experimental apparatus. Appl. Energy 262, 114397.
Wang, S., Luo, D., Zhang, X., Lu, X., Shi, Y., 2018. Experimental study of mechanical properties of hydrate clay. J. Exp. Mech. 33, 245–252, (in Chinese with English abstract).
Wei, J., Fang, Y., Lu, H., Lu, H., Lu, J., Liang, J., Yang, S., 2018. Distribution and characteristics of natural gas hydrates in the shenhu sea area, south China sea. Mar. Pet. Geol. 98, 622–628.
Wei, J., Liang, J., Lu, J., Zhang, W., He, Y., 2019. Characteristics and dynamics of gas hydrate systems in the northwestern south China sea - results of the fifth gas hydrate drilling expedition. Mar. Pet. Geol. 110, 287–298.
Wei, J., Pape, T., Sultan, N., Colliat, J.L., Himmler, T., Ruffine, L., de Prunelé, A., Dennielou, B., Garziglia, S., Marsset, T., Peters, C.A., Rabiu, A., Bohrmann, G., 2015. Gas hydrate distributions in sediments of pockmarks from the Nigerian margin - results and interpretation from shallow drilling. Mar. Pet. Geol. 59, 359–370.
Wei, J., Wu, T., Zhu, L., Fang, Y., Liang, J., Lu, H., Cai, W., Xie, Z., Lai, P., Cao, J., Yang, T., 2021. Mixed gas sources induced co-existence of si and sII gas hydrates in the Qiongdongnan Basin, South China Sea. Mar. Pet. Geol. 128, 105024.
Yang, S., Liang, J., Lei, Y., Gong, Y., Xu, H., Wang, H., Lu, J., Melanie, H., Peter, S., Wei, J., 2017. GMGS4 gas hydrate drilling expedition in the South China Sea. Fire Ice 17, 7–11.
Yang, S., Zhang, M., Liang, J., 2015. Preliminary results of China's third gas hydrate drilling expedition: A critical step from discovery to development in the south China sea. Fire Ice: Methane Hydrate Newsl. 15, 1–5.
Ye, J., Qin, X., Qiu, H., Liang, Q., Dong, Y., Wei, J., Lu, H., Lu, J., Shi, Y., Zhong, C., Xia, Z., 2018. Preliminary results of environmental monitoring of the natural gas hydrate production test in the south China sea. China Geol. 1, 202–209.
Ye, J., Qin, X., Xie, W., Lu, H., Ma, B., Qiu, H., Liang, J., Lu, J., 2020. Main progress of the second gas hydrate trial production in the south China sea. Geol. China 47, 557–568, (in Chinese with English abstract).
Ye, J., Wei, J., Liang, J., Lu, J., Lu, H., Zhang, W., 2019. Complex gas hydrate system in a gas chimney, south China sea. Mar. Pet. Geol. 104, 29–39.
Yoneda, J., Hyodo, M., Nakata, Y., Yoshimoto, N., 2010. Triaxial shear characteristics of methane hydrate-bearing sediment in the deep seabed. J. Geotech. Eng. Jpn. III 66, 742–756.
Yoneda, J., Masui, A., Konno, Y., Jin, Y., Egawa, K., Kida, M., Ito, T., Nagao, J., Tenma, N., 2015a. Mechanical behavior of hydrate-bearing pressure core sediments visualized under tri-axial compression. Mar. Pet. Geol. 66, 451–459.
Yoneda, J., Masui, A., Konno, Y., Jin, Y., Egawa, K., Kida, M., Ito, T., Nagao, J., Tenma, N., 2015b. Mechanical properties of hydrate-bearing turbidite reservoir in the first gas production test site of the eastern nankai trough. Mar. Pet. Geol. 66, 471–486.
Yoneda, J., Masui, A., Konno, Y., Jin, Y., Kida, M., Katagiri, J., Nagao, J., Tenma, N., 2017. Pressure-core-based reservoir characterization for geomechanics: insights from gas hydrate drilling during 2012-2013 at the eastern nankai trough. Mar. Pet. Geol. 86, 1–16.
Yoneda, J., Oshima, M., Kida, M., Kato, A., Konno, Y., Jin, Y., Jang, J., Waite, W.F., Kumar, P., Tenma, N., 2019a. Permeability variation and anisotropy of gas hydrate-bearing pressure-core sediments recovered from the krishna–godavari basin, offshore India. Mar. Pet. Geol. 108, 524–536.
Yoneda, J., Oshima, M., Kida, M., Kato, A., Konno, Y., Jin, Y., Jang, J., Waite, W.F., Kumar, P., Tenma, N., 2019b. Pressure core based onshore laboratory analysis on mechanical properties of hydrate-bearing sediments recovered during India's national gas hydrate program expedition (NGHP) 02. Mar. Pet. Geol. 108, 482–501.
Zhang, W., Liang, J., Lu, J., Wei, J., Su, P., Fang, Y., Guo, Y., Yang, S., Zhang, G., 2017. Accumulation mechanisms of high saturation natural gas hydrate in Shenhu Area, northern South China Sea. Pet. Explor. Dev. 44, 1–11, (in Chinese with English abstract).
Zhang, W., Liang, J., Wei, J., Lu, J.a., Su, P., Lin, L., Huang, W., Guo, Y., Deng, W., Yang, X., Wan, Z., 2020. Geological and geophysical features of and controls on occurrence and accumulation of gas hydrates in the first offshore gas-hydrate production test region in the shenhu area, northern south China sea. Mar. Pet. Geol. 114, 104191.

Zhang, X., Lu, X., Chen, X., Zhang, L., Shi, Y., 2016. Mechanism of soil stratum instability induced by hydrate dissociation. Ocean Eng. 122, 74–83.
Zhang, X., Lu, X., Li, P., 2019. A comprehensive review in natural gas hydrate recovery methods. Sci. Sin. Phys. Mech. Astron. 49, 034604, (in Chinese with English abstract).
Zhang, X., Lu, X., Shi, Y., Xia, Z., 2015a. Study on the mechanical properties of hydrate-bearing silty clay. Mar. Pet. Geol. 67, 72–80.
Zhang, X., Lu, X., Shi, Y., Xia, Z., Liu, W., 2015b. Centrifuge experimental study on instability of seabed stratum caused by gas hydrate dissociation. Ocean Eng. 105, 1–9.
Zhang, X., Luo, D., Lu, X., Liu, L., Liu, C., 2018. Mechanical properties of gas hydrate-bearing sediments during hydrate dissociation. Acta Mech. Sinica 34, 266–274.
Zhu, C., Cheng, S., Li, Q., et al., 2019. Giant submarine landslide in the south China sea: Evidence, causes and implications. J. Mar. Sci. Eng. 7 (152).
Zhu, C., Jiao, X., Cheng, S., Li, Q., Liu, K., Shan, H., Li, C., Jia, Y., 2020. Visualizing fluid migration due to hydrate dissociation: Implications for submarine slides. Environ. Geotech. http://dx.doi.org/10.1680/jenge.19.00068.